JOC The Journal of Organic Chemistry

Article

pubs.acs.org/joc

[4 + 2] Cycloaddition Reaction To Approach Diazatwistpentacenes: Synthesis, Structures, Physical Properties, and Self-assembly

Junbo Li,[†,‡] Peizhou Li,[§] Jiansheng Wu,[†] Junkuo Gao,[∥] Wei-Wei Xiong,[†] Guodong Zhang,[†] Yanli Zhao,[§] and Qichun Zhang*[,†]

[†]School of Materials Science and Engineering, Nanyang Technological University, Singapore 639798, Singapore

[‡]School of Chemistry and Environmental Engineering, Wuhan Institute of Technology, Wuhan 430074, China

[§]Division of Chemistry and Biological Chemistry, School of Physical and Mathematical Sciences, Nanyang Technological University, Singapore 637459, Singapore

[∥]College of Materials and Textile, Zhejiang Sci-Tech University, Hangzhou 310018, China

Supporting Information

ABSTRACT: Three novel diazatwistpentacenes (1,4,6,13-tetraphenyl-7:8,11:12-bisbenzo-2,3-diazatwistpentacene (**1**, IUPAC name: 9,11,14,16-tetraphenyl-1,6-dihydrobenzo[8,9]triphenyleno[2,3-*g*]phthalazine); 1,4-di(pyridin-2-yl)-6,13-diphenyl-7:8,11:12-bisbenzo-2,3-diazatwistpentacene (**2**, IUPAC name: 9,16-diphenyl-11,14-di(pyridin-2-yl)-1,6-dihydrobenzo[8,9]triphenyleno[2,3-*g*]phthalazine); and 1,4-di(thien-2-yl)-6,13-diphenyl-7:8,11:12-bisbenzo-2,3-diazatwistpentacene (**3**, IUPAC name: 9,16-diphenyl-11,14-di(thien-2-yl)-1,6-dihydrobenzo[8,9]triphenyleno-[2,3-*g*]phthalazine)) have been successfully synthesized through [4 + 2] cycloaddition reaction involving *in situ* arynes as dienophiles and substituted 1,2,4,5-tetrazines as dienes. Their structures have been determined by single-crystal X-ray diffraction, confirming that all compounds have twisted configurations with torsion angles between the pyrene unit and the 2,3-diazaanthrance part as high as 21.52° (for **1**), 24.74° (for **2**), and 21.14° (for **3**). The optical bandgaps for all compounds corroborate the values derived from CV. The calculation done by DFT shows that the HOMO−LUMO bandgaps are in good agreement with experimental data. Interestingly, the substituted groups (phenyl, pyridyl, thienyl) in the 1,4-positions did affect their self-assembly and the optical properties of as-resulted nanostructures. Under the same conditions, compounds **1**−**3** could self-assemble into different morphologies such as microrods (for **1**), nanoprisms (for **2**), and nanobelts (for **3**). Moreover, the UV−vis absorption and emission spectra of as-prepared nanostructures were largely red-shifted, indicating J-type aggregation for all materials. Surprisingly, both **1** and **2** showed aggregation-induced emission (AIE) effect, while compound **3** showed aggregation-caused quenching (ACQ) effect. Our method to approach novel twisted azaacenes through [4 + 2] reaction could offer a new tool to develop unusual twisted conjugated materials for future optoelectronic applications.

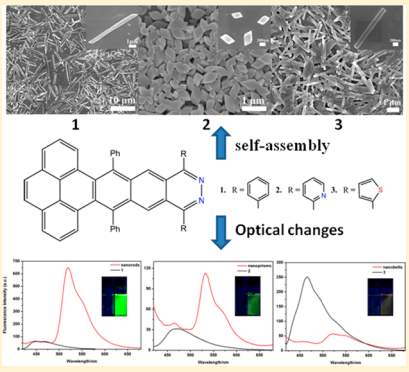

INTRODUCTION

Integrating pyrene species into the backbones of oligoacenes[1−3] would make the resulting frameworks twisted, and this type of materials (namely twistacenes)[4−6] has great potential applications in organic semiconductor devices. If some CH groups in the backbone of oligotwistacenes are replaced by N atoms, these compounds will become oilgotwistazaacenes.[7−12] In fact, some oligoazaacenes have been demonstrated as promising materials for ion sensing, OLED, FET, memory devices, phototransistors, and solar cells.[7−12]

Although azaacenes could be prepared through several methods[7c,8a] (e.g., S_N2 reaction between diamines and dihydroxy (or dihalo) compounds following by oxidation, or condensation between diamine (or tetraamine) and diketone (or tretraketone)), new methods are still required to approach larger azaacenes ($n > 6$) because all current methods involve byproduct water,[7−10] which could react with targeted azaacenes and switch the configuration of N atoms from sp^2 to sp^3.[13] Since oligoacenes can be conveniently prepared through [4 + 2] reactions involving arynes as dienophiles,[5,6] this type of reaction should be a promising method to construct larger azaacenes. In this report, we demonstrate that larger diazatwistpentacenes can be prepared through [4 + 2] reaction between 3,6-disubstituted 1,2,4,5-tetrazines as dienes and *in situ* arynes as dienophiles (from 1,4′-diphenyl-naphtho-(2.3:1.2)-pyrene-6-amino-7′-carboxylate acid).[6] In addition, we also investigate how different substitution groups (e.g., phenyl, pyridyl, thienyl) in 1-/4-positions on the backbones of 6,13-diphenyl-7:8,11:12-bisbenzo-2,3-diazatwistpentacene (IUPAC name: 9,11,14,16-tetraphenyl-1,6-dihydrobenzo[8,9]-triphenyleno[2,3-*g*]phthalazine) affect their assembly and the morphologies/properties of the resulting nanoparticles since the self-assembly of organic semiconductor molecules into

Received: February 19, 2014
Published: April 17, 2014

   dx.doi.org/10.1021/jo500400d | *J. Org. Chem.* 2014, 79, 4438−4445

micro/nanostructures is very important to tune their optical properties as well as for device performance.[14] Our results clearly show that the different substituent groups at 1-/4-positions have a big effect on optical properties and the shape/size of the resulting particles.

RESULTS AND DISCUSSION

Synthesis, Characterization, and Crystal Structures. The general synthetic approach to compounds **1**−**3** is shown in Scheme 1. Compound **4** was synthesized in five steps according to the reported method,[6a] and the target compounds **1**−**3** were prepared through a [4 + 2] cycloaddition reaction involving *in situ* arynes as dienophiles (from precursor **4** reacting with isoamyl nitrite) and 3,6-diphenyl-1,2,4,5-tetrazine, 3,6-di(pyridin-2-yl)-1,2,4,5-tetrazine, or 3,6-di(thien-2-yl)-1,2,4,5-tetrazine as dienes (Scheme 1), respectively. All new compounds were fully characterized by ^{1}H NMR, ^{13}C NMR, and HR-MS. Moreover, the structures of compounds **1**−**3** were furthermore confirmed by single crystal structure analysis. The as-prepared compounds **1**−**3** could be dissolved in common organic solvents such as methylene chloride, chloroform, tetrahydrofuran (THF), *o*-dichlorobenzene (ODCB), and *N*,*N*-dimethylformide.

Scheme 1. Synthetic Routes of Compounds 1−3

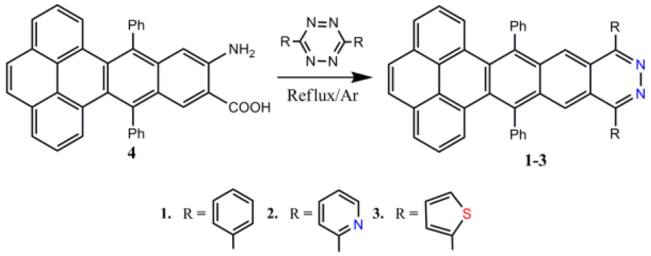

To investigate the effects of substitution groups on the molecular packing arrangement in the solid state, the single crystals of compounds **1**−**3** were grown by slow evaporation of dichloromethane/methanol (1:1) mixed solutions in room temperature. As shown in Figure 1, all compounds display significantly twisted structures. Compound **1** possesses a triclinic space group *P*-1. Its unit cell data are as follows: a = 10.9885(4) Å, b = 11.6518(4) Å, c = 15.3264(6) Å, α = 85.39(0)°, β = 89.27(0)°, γ = 73.76(0)°. The torsion angle between pyrene unit and 2,3-diazaanthrance part is about 21.52° (C_{13}−C_{26}−C_{12}−C_{25}), which is smaller than the reported

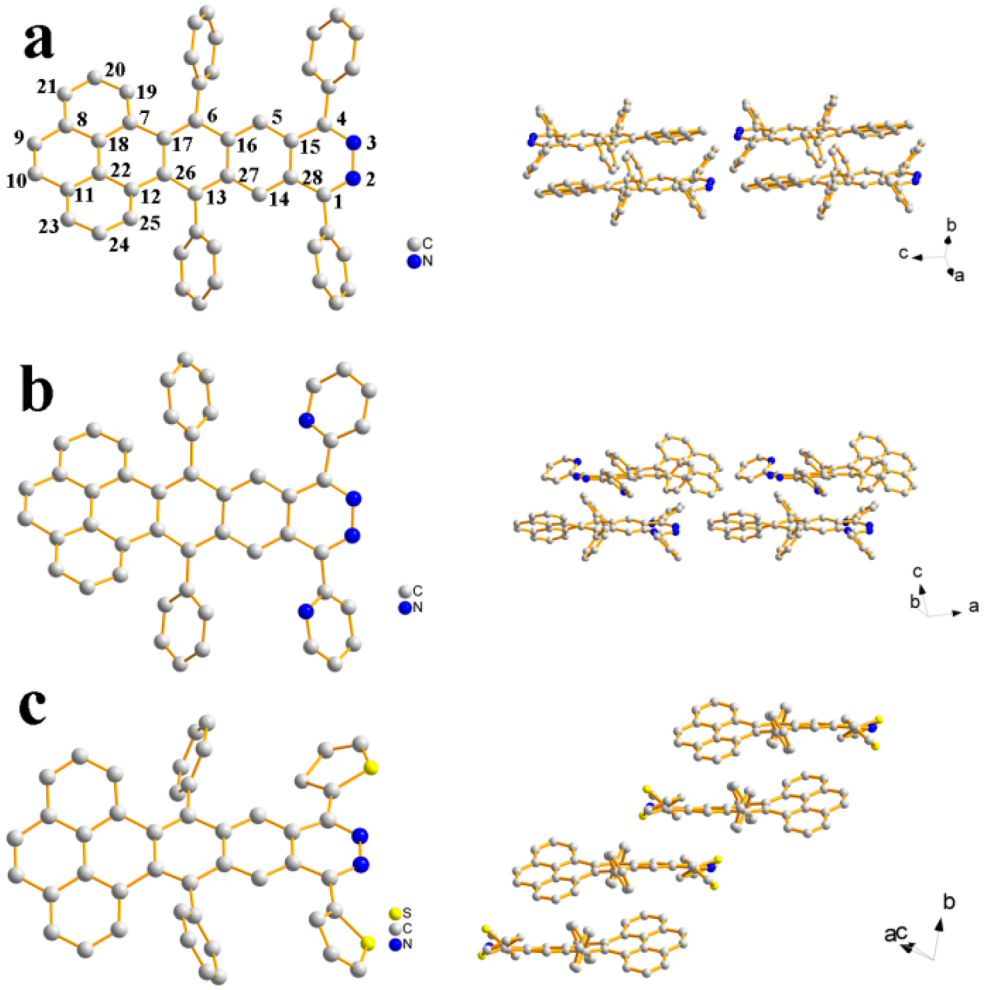

Figure 1. (a) Crystal structure of compound **1** (hydrogen atoms and the solvent CH_2Cl_2 are omitted) and the crystal packing arrangement. (b) Crystal structure of compound **2** (hydrogen atoms are omitted) and the crystal packing arrangement. (c) Crystal structure of compound **3** (hydrogen atoms are omitted) and the crystal packing arrangement.

dx.doi.org/10.1021/jo500400d | J. Org. Chem. 2014, 79, 4438−4445

twistpentacene.[6b] Moreover, the lengths of the $C_{17}-C_7$ and $C_{26}-C_{12}$ bonds are 1.49 and 1.48 Å, which are longer than the rest of the C−C bonds. Additionally, the individual molecules are stacked in head-to-tail mode. There are weak $\pi-\pi$ stacking interactions between the pyrene unit and the 2,3-diazaanthrance part, and the distance between them is nearly 4.02 Å (Supplementary Figure S1). When the substituted groups at 1-/4-positions were changed into pyridyl groups, a large unit cell (monoclinic) with space group of $C2/c$ for compound **2** was obtained. Its unit cell data are as follows: a = 26.9975(6) Å, b = 14.9487(3) Å, c = 16.8201(4) Å, β = 99.47(0)°. The torsion angle is about 24.74°, which is larger than that of compound **1**. The individual molecules stacking in the crystal of compound **2** also adopt head-to-tail mode. Interestingly, there is no stacking between the pyrene unit and the 2,3-diazaanthrance part; instead, there are weak $\pi-\pi$ stacking interactions between 2,3-diazaanthrance units. The distance between two neighboring 2,3-diazaanthrance units is nearly 4.02 Å (Supplementary Figure S2), which could explain the larger unit cell for compound **2**. When the substituted groups in 1-/4-positions are replaced by 2-thienyl, compound **3** is obtained and has a triclinic space group P-1. Its unit cell data are as follows: a = 10.3831(6) Å, b = 13.0198(5) Å, c = 13.2997(6) Å, α = 81.76(0)°, β = 78.2(0)°, γ = 70.81(0)°. The torsion angle is about 21.14°, which is similar to that of compound **1** but smaller than that of compound **2**. There are two major intermolecular interactions stabilizing the crystal packing in compound **3**. The first one is the weak $\pi-\pi$ stacking interactions between the pyrene piece and the 2,3-diazaanthrance unit, and the other is the weak $\pi-\pi$ stacking interactions between two 2,3-diazaanthrance units (Figure 1c). The distance between them is nearly 3.88 Å (Supplementary Figure S3). Such arrangement might come from the smaller space hindrance of thienyl groups.

Different Optical and Electrochemical Properties. The UV−vis absorption spectra of compounds **1**−**3** were recorded in THF at room temperature. As shown in Figure 2, in the low

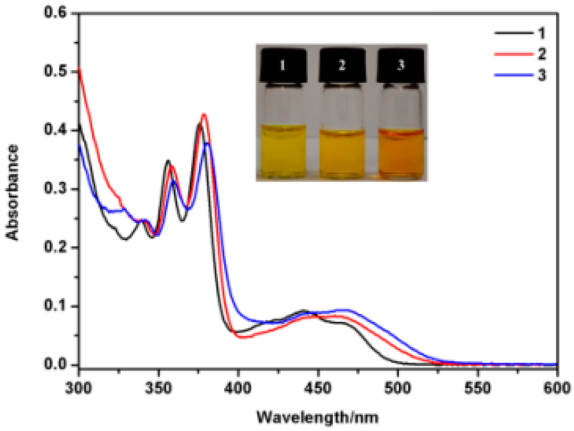

Figure 2. UV−vis spectra of compounds **1**−**3** (1×10^{-5} M) in THF. The inset shows the color of compounds **1**−**3** (1×10^{-3} M) in THF.

energy region, the absorption peak of compound **1** is at 441 nm with a shoulder at 465 nm. In the high energy region, there are three peaks at 338, 356, and 376 nm, respectively. The λ_{max}^{onset} is nearly 500 nm (Supplementary Figure S4), which is similar to the parent twistpentacene.[6b] When the substituted groups at 1-/4-positions were changed from phenyl to pyridyl (**2**) or thienyl (**3**), the number and shape of absorption peaks have no obvious changes, but all peaks are red-shifted. Four absorption peaks for compound **2** appear at 341, 358, 378, and 464 nm, while compound **3** has more red-shifted absorption peaks at 342, 359, 381, and 471 nm, respectively. Such red-shifts may be a result of the enhancement of an intramolecular charge transfer (ICT) process with the replacement of electron-withdrawing groups (pyridyl group) or electron-donating groups (thienyl groups) at 1-/4-positions. Meanwhile, the color of the solutions change from yellow to dark yellow (Figure 2, inset). Unlike the parent twistpentacene, which shows high fluorescence (Φ_f = 0.69 in CH_2Cl_2),[6b] all as-prepared diazatwistpentacenes show very weak fluorescence (Figure 3), which indicates that the substitution of N atoms in

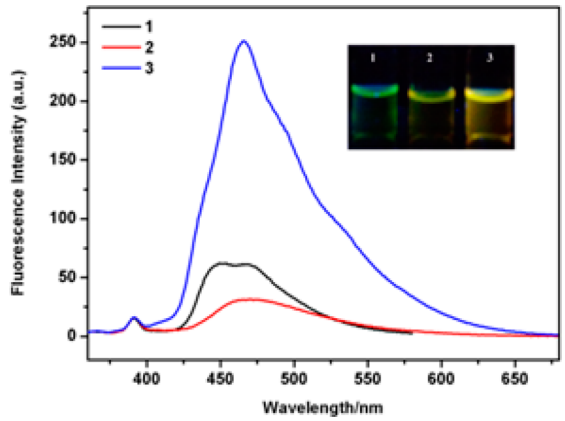

Figure 3. Fluorescence spectra of compounds **1**−**3** (1×10^{-5} M) in THF. The inset shows the fluorescence color of compounds **1**−**3** (1×10^{-3} M) in THF. Excitation wavelength is 350 nm.

2-/3-positions will strongly quench the fluorescence. Actually, the weak fluorescence behavior is common for 1,2-diazine-containing molecules, which is possibly caused by the intersystem crossing effect.[15] The fluorescence quantum yield of compound **1** in THF is 0.0028, using quinine sulfate dehydrate as the standard (Φ_f = 0.58 in 0.1 M H_2SO_4),[16] while pyridyl groups in 1-/4-positions induce a red-shift fluorescence with a lower intensity (Φ_f = 0.0020). Interestingly, thienyl groups (**3**) can slightly enhance the fluorescence intensity (Φ_f = 0.0063) compared to phenyl (**1**) and pyridyl groups (**2**). The possible reason is that thienyl group is a stronger electron-donating group than phenyl and pyridyl groups, which can increase electron density of the conjugated system and induce a stronger fluorescence.[15a] The fluorescence differences are also confirmed by simulated fluorescence spectra (Supplementary Figure S6). These results clearly suggest that different substituent groups at 1-/4-positions did affect the optical properties of diazatwistpentacenes.

The electrochemical properties of compounds **1**−**3** were studied in a three-electrode electrochemical cell with tetrabutylammonium hexafluorophosphate (Bu_4NPF_6, TBAF) (0.1 M) as an electrolyte and Ag/AgCl as a reference electrode (Figure 4 and Table 1). All compounds show two reversible reduction peaks and two irreversible oxidation peaks. The onset oxidative potentials for compounds **1**−**3** were measured as 1.34, 1.23, and 1.30 V, respectively. On the basis of the equation HOMO = $-E_{onset}^{ox}$ − 4.4 eV,[10a] the HOMO energy levels for **1**−**3** were calculated as −5.74, −5.63, and −5.70 eV, respectively. Meanwhile, the LUMO energy levels for compounds **1**−**3** were calculated to be −3.23, −3.30, and

dx.doi.org/10.1021/jo500400d | J. Org. Chem. 2014, 79, 4438−4445

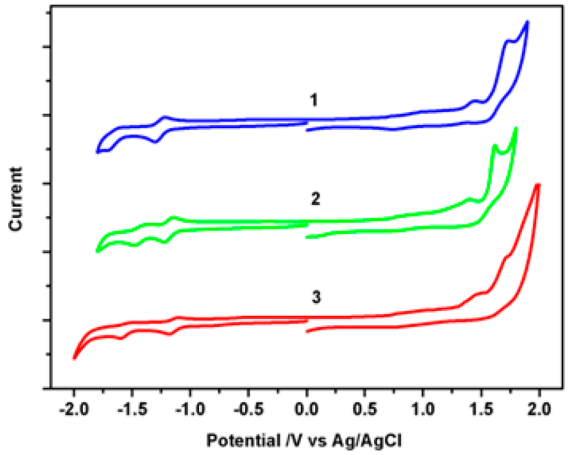

Figure 4. Cyclic voltammetry curves of **1**−**3** in CH_2Cl_2 solution containing 0.1 M TBAP electrolyte. Scanning rate: 100 mV/s.

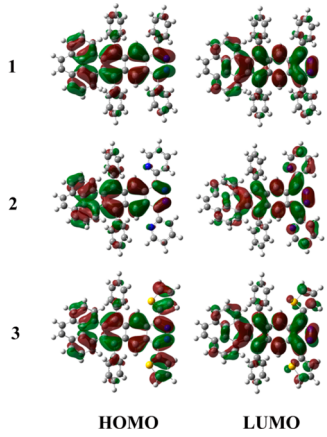

Figure 5. Wave functions for the HOMO and LUMO of compounds **1**−**3**.

−3.38 eV, respectively. It is worth noting that the change of the substituent groups from phenyl to pyridyl and thienyl groups induces an increase of HOMO energy level but causes a decrease of LUMO energy level, which results in the smaller bandgaps of compounds **2** and **3** compared with that of compound **1**.

The molecular geometries of compound **1**−**3** were optimized using density functional theory (DFT) at the B3LYP/6-31G* level.[17] The ground state frontier molecular orbitals of the optimized molecules were also calculated at the same level. As shown in Figure 5, both the highest occupied molecular orbital (HOMO) and lowest unoccupied molecular orbital (LUMO) of compound **1** are mainly localized on the pyrene units and 2,3-diazaanthrance parts. When phenyl groups at 1-/4-positions were replaced by pyridyl groups, the HOMO orbital still mainly localized on the pyrene units and 2,3-diazaanthrance parts, but the LUMO orbital localized on pyrene, 2,3-diazaanthrance, and pyridyl groups, respectively. For compound **3**, except for the localization on pyrene units and 2,3-diazaanthrance parts, the HOMO orbital also localized on thienyl groups, while the LUMO orbital mainly localized on the pyrene units and 2,3-diazaanthrance parts. The calculated HOMO and LUMO orbital energy levels were summarized in Table 1.

Self-Assembly and Optical Changes. Since self-assembly is a very interesting phenomenon, which can be investigated to understand the behaviors and properteis of as-prepared materials in micro/nanoscale,[14] it is highly desirable for us to do some research in this direction. Currently, organic nanostructures can be obtained through hard/soft templates,[18] reprecipitation,[19] chemical reaction,[20] laser ablation,[21] electrochemical methods,[22] and seed-induced growth[23] through weak interactions such as hydrogen bonding, $\pi-\pi$ stacking, electrostatic interaction, and hydrophobic interaction. Among them, the reprecipitation with the help of surfactants might be one of the most convient methods. In our research, the self-assembly of compounds **1**−**3** was realized through the addition of a THF solution of compounds **1**−**3** (10^{-3} M, 1 mL) into an aqueous solutions containing P123 block polymers (1 mg/mL, 5 mL) as the surfactant. Interestingly, the change of the substituted groups at 1-/4-positions has large effect on the self-assembled structures. Compounds **1**−**3** readily form different nano/microstructures as microrods, nanoprisms, and nanobelts, respectively (Figure 6). As shown in Figure 6a, compound **1** forms microrods with diameters in the range of 550 nm to 1.2 μm and lengths of 3−10 μm. The XRD patterns (Figure 6b) further confirmed that the as-prepared microrods are single crystals and the preferential orientation is the (001) lattice plane. However, when phenyl groups in 1-/4-positions are replaced by pyridyl groups, the self-assembled structure dramatically changed from microrods to nanoprisms. As shown in Figure 6c, the as-prepared nanoprisms have widths between 250 and 550 nm and lengths between 200 and 390 nm. Meanwhile, the powder XRD spectrum shows that the as-obtained nanostructures have the same pattern as the simulated one, which indicated that the self-assembled nanoprisms are crystalline and show phase purity. Moreover, when the 1-/4-positions are changed with thienyl groups, larger areas of nanobelts with diameters of 120−190 nm and lengths of 1−2 μm were formed. Actually, the self-assembly of compounds **1**−**3** without P123 was also investigated. As shown in Supplementary Figure S7, compounds **1** and **2** cannot form uniform nanostructure in aqueous solution, while compound **3** can form large-scale quadrangles with diameters between 300 and 400 nm and lengths of 1−2.3 μm. These results suggest that the soft-template P123 is a key for the control of the shape and size during self-assembly. The possible self-assembly

Table 1. Optical and Electrochemical Data of Compounds 1−3

compd	E_{onset}^{red} (V)[a]	E_{onset}^{ox} (V)[a]	E_{gap} (eV)[b]	LUMO (eV)[c]	HOMO (eV)[d]	E_{gap}/λ_{onset} (eV/nm)[e]	LUMO (eV)[f]	HOMO (eV)[f]	E_{gap} (eV)[f]	$\varepsilon_{max}/\lambda_{max}$ (10^3 M^{-1} cm^{-1}/nm)	λ_{em} (nm)[g]	Φ_f
1	−1.17	1.34	2.51	−3.23	−5.74	2.51/494	−2.34	−5.31	2.97	9.3/441	450	0.0028
2	−1.10	1.23	2.33	−3.30	−5.63	2.41/515	−2.35	−5.16	2.81	8.3/464	472	0.0020
3	−1.02	1.30	2.32	−3.38	−5.70	2.37/523	−2.41	−5.24	2.83	9.1/471	466	0.0063

[a]Obtained from cyclic voltammograms in CH_2Cl_2. Reference electrode was Ag/AgCl. [b]$E_{gap} = E_{onset}^{ox} - E_{onset}^{red}$. [c]Calculated according to the formula $E_{LUMO} = E_{HOMO} + E_{gap}$. [d]Calculated from cyclic voltammograms. [e]Optical band gap, $E_{gap} = 1240/\lambda_{onset}$. [f]Obtained from theoretical calculations. [g]Excitation wavelength was 350 nm.

dx.doi.org/10.1021/jo500400d | J. Org. Chem. 2014, 79, 4438−4445

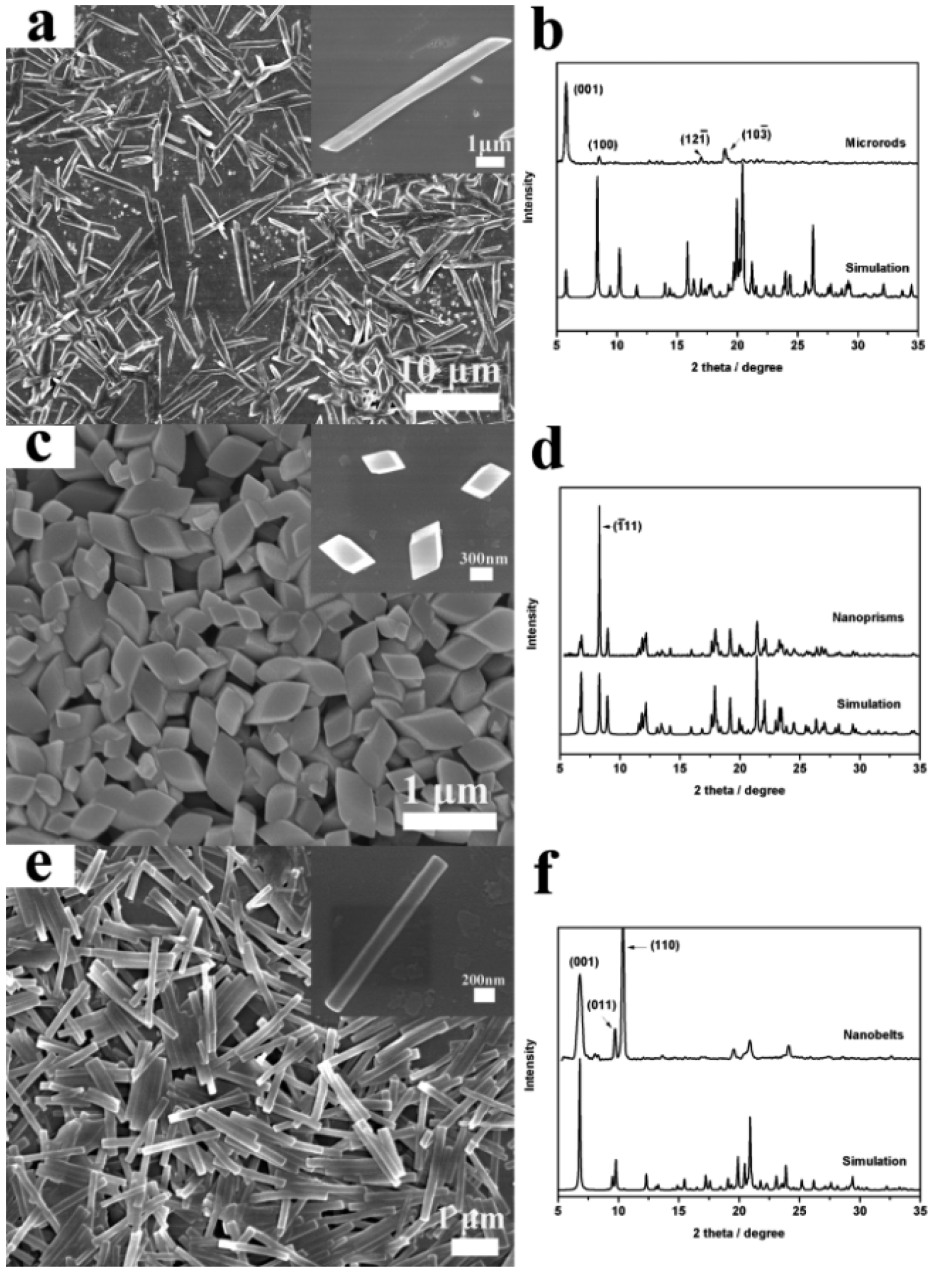

Figure 6. (a) SEM image of compound **1** with micrororods. (b) XRD patterns of microrods. (c) SEM image of compound **2** with nanoprisms. (d) XRD patterns of nanoprisms. (e) SEM image of compound **3** with nanobelts. (e) XRD patterns of nanobelts.

processes are proposed as follows: THF is a good solvent and water is a poor solvent for compounds **1**−**3**. When THF solutions are injected into the aqueous solution containing P123, compounds **1**−**3** tend to aggregate to form crystalline micro/nanostructures due to intermolecular π−π stacking and the hydrophobic effect.[24] Meanwhile, the different packing in single crystal structures of compounds **1**−**3** could explain the formation of different nano/microstructures during self-assembly under the same conditions.

The UV−vis spectra of compounds **1**−**3** in THF solution and the related microrods, nanoprisms, and nanobelts in aqueous solution are shown in Figure 7a. The UV−vis absorption of all nanostructures become broad and drastically red-shifted compared to those of **1**−**3** in THF solution. The microrods (formed from **1**) and nanobelts (formed from **3**) have three similar absorption peaks at 393, 467, 499 nm (microrods) and 395, 480, 505 nm (nanobelts), respectively. However, nanoprisms (formed from **2**) show broader peaks and a larger red-shift with one absorption peak at 545 nm. The red-shifts of absorption peaks for all particles suggest J-type aggregations.[25] More interestingly, in THF solution, compounds **1**−**3** show very weak fluorescence with fluorescence quantum yields of 0.0028, 0.0020 and 0.0063, respectively. After self-assembly, the emission wavelengths were all red-shifted but the emission strength changes were different. Compounds **1** and **2** showed obvious aggregation-induced emission (AIE) effects,[26] and the fluorescence quantum yields were increased to 0.0140 and 0.0059 with nanostructures dispersed in aqueous solutions. It should be noted that the fluorescence quantum yield of microrods is 4.1 times higher than that of compound **1** in THF. However, compound **3** shows aggregation-caused quenching (ACQ)[27] effect, and the

dx.doi.org/10.1021/jo500400d | J. Org. Chem. 2014, 79, 4438−4445

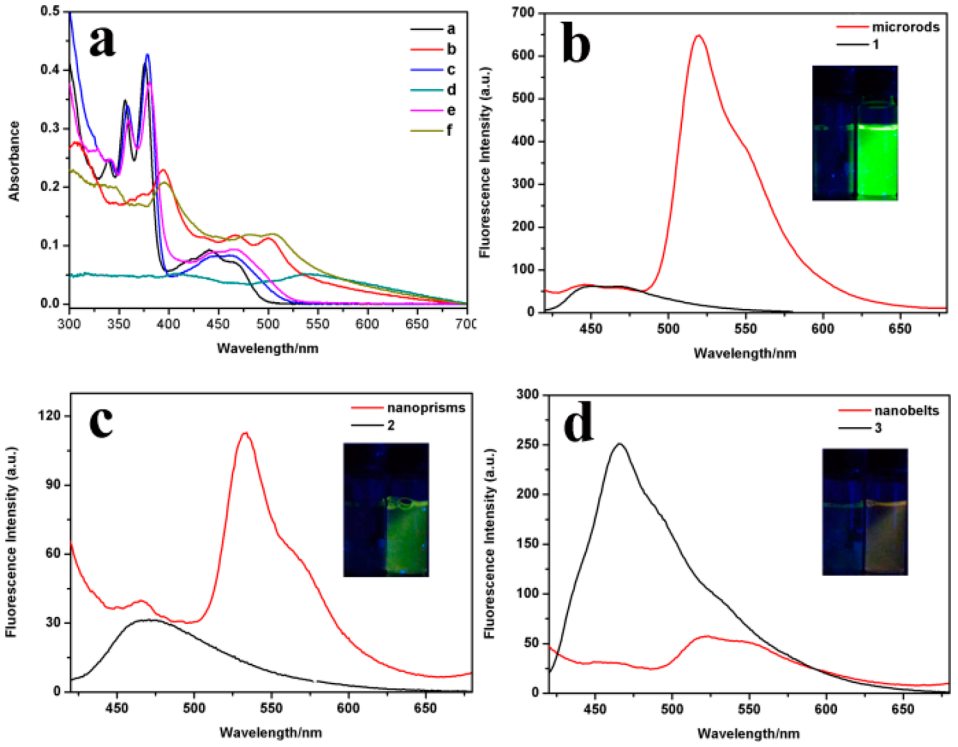

Figure 7. (a) UV−vis spectra: compound **1** in THF solution (a), microrods (formed by **1**) dispersed in aqueous solution (b), compound **2** in THF solution (c), nanoprisms (formed by **2**) dispersed in aqueous solution (d), compound **3** in THF solution (e), and nanobelts (formed by **3**) dispersed in aqueous solution (f). Fluoroescence spectra: (b) compound **1** in THF and the microrods in aqueous solution; (c) compound **2** in THF and the nanoprisms in aqueous solution; and (d) compound **3** in THF and the nanobelts in aqueous solution. Excitation wavelength is 350 nm.

fluorescence quantum yields was decreased to be 0.0034. The AIE effects in self-assembled particles for compounds **1** and **2** might have some potential applications as biosensors.

CONCLUSIONS

In summary, we have successfully synthesized three novel diazatwistpentacene derivatives through [4 + 2] cycloaddition reactions, and the as-prepared compounds have been fully characterized. Our results showed that different substitution groups at the 1-/4-positions have large effects on the optical properties, single crystal packing, and corresponding self-assembly. The self-assembly of compounds **1**−**3** showed completely different nano/microstructures, which have different optical properties in aqueous solutions. Our synthetic method as well as the obtained information from the effect of different substitution groups at the 1-/4-positions on the properties of diazatwistpentacene derivatives could offer a guideline to prepare novel larger azaacenes.

EXPERIMENTAL SECTION

General Procedures. All chemicals were used directly without further purification. Ultrapure water was obtained from the Millipore S. A. 67120 apparatus with a resistivity of 18.2 MΩ cm.

Optical Study. A 1.0-cm quartz cuvette in a volume of 3.0 mL was used for all spectra collection. Unless otherwise noted, for all measurements the excitation wavelength was at 350 nm. The slit width of excitation was 5.0 nm, and the slit width of emission was 5.0 nm.

Self-Assembly. One milliliter of THF solution (1 mM **1**) was injected into 5 mL of water containing P123 with strong stirring. After continuously stirring for 15 min, the obtained solution was aged overnight to give microrods. The similar method is used for self-assembling compounds **2** and **3**.

Preparation of SEM Samples. One drop of the solution (20 μL) was put on a silica wafer and dried over 12 h. The as-prepared samples were then coated with gold in an ion coater for 40 s.

Synthesis. *Compound 1.* Under an atmosphere of dry argon, 3,6-diphenyl-1,2,4,5-tetrazine (182 mg, 0.78 mmol) and an excess of isoamyl nitrite (1 mL) were added into 30 mL of 1,2-dichloroethane. The mixture was heated to reflux, and then the corresponding acid **4** (400 mg, 0.78 mmol) dispersed in 20 mL of 1,2-dichloroethane was added to the mixture dropwise. After addition, the mixture was kept refluxing overnight. Then, the mixture was cooled to room temperature, and the solvent was removed under reduced pressure. The resultant residue was purified by silica gel column chromatography using CH_2Cl_2/CH_3OH (80/1, v/v) as eluent to afford compound **1** as a yellow solid (154 mg, 30%). Mp: >300 °C. ^{1}H NMR ($CDCl_3$, 300 MHz) δ: 7.34 (t, 2H, J = 7.8 Hz), 7.49−7.53 (m, 16H), 7.80−7.90 (m, 10H), 8.80 (s, 2H). ^{13}C NMR ($CDCl_3$, 75 MHz) δ: 122.2, 125.0, 126.8, 126.9, 127.0, 128.0, 128.3, 129.2, 129.3, 129.4, 129.7, 130.1, 130.9, 131.2, 132.1, 133.6, 136.4, 137.1, 141.2, 159.4. HRMS (ESI-TOF) m/z: $[M + H]^+$ calcd for $C_{50}H_{31}N_2$ 659.2487, found 659.2489. Anal. Calcd for $C_{50}H_{30}N_2$: C, 91.16; H, 4.59; N, 4.25. Found: C, 91.04; H, 4.70; N, 4.16.

Compound 2. Under an atmosphere of dry argon, 3,6-di(pyridin-2-yl)-1,2,4,5-tetrazine (184 mg, 0.78 mmol) and an excess of isoamyl nitrite (1 mL) were added into 30 mL of 1,2-dichloroethane. The mixture was heated to reflux, and then the corresponding acid **4** (400 mg, 0.78 mmol) dispersed in 20 mL of 1,2-dichloroethane was added to the mixture dropwise. After addition, the mixture was kept refluxing overnight. Then, the mixture was cooled to room temperature, and the solvent was removed under reduced pressure. The resultant residue was purified by silica gel column chromatography using CH_2Cl_2/CH_3OH (60/1, v/v) as eluent to afford compound **2** as a brown solid (113 mg, 22%). Mp: >300 °C. ^{1}H NMR ($CDCl_3$, 300 MHz) δ: 7.32 (t, 2H, J = 7.8 Hz), 7.38−7.42 (m, 2H), 7.54−7.64 (m, 10H), 7.87−7.93 (m, 8H), 8.31 (d, 2H, J = 9 Hz), 8.65 (d, 2H, J = 9 Hz), 9.73 (s, 2H). ^{13}C NMR ($CDCl_3$, 75 MHz) δ: 122.0, 123.8, 125.0, 125.4, 126.3, 126.8, 126.9, 127.7, 127.8, 129.1, 129.6, 129.9, 130.8, 131.2, 132.6,

dx.doi.org/10.1021/jo500400d | J. Org. Chem. 2014, 79, 4438−4445

133.7, 136.9, 137.5, 141.5, 148.4, 156.2, 156.8. HRMS (ESI-TOF) m/z: $[M + H]^+$ calcd for $C_{48}H_{29}N_4$ 661.2392, found 661.2391. Anal. Calcd for $C_{48}H_{28}N_4$: C, 87.25; H, 4.27; N, 8.48. Found: C, 87.40; H, 4.35; N, 8.38.

Compound **3**. Under an atmosphere of dry argon, 3,6-di(thiophen-2-yl)-1,2,4,5-tetrazine (192 mg, 0.78 mmol) and an excess of isoamyl nitrite (1 mL) were added into 30 mL of 1,2-dichloroethane. The mixture was heated to reflux, and then the corresponding acid **4** (400 mg, 0.78 mmol) dispersed in 20 mL of 1,2-dichloroethane was added to the mixture dropwise. After addition, the mixture kept refluxing overnight. Then, the mixture was cooled to room temperature, and the solvent was removed under reduced pressure. The resultant residue was purified by silica gel column chromatography using CH_2Cl_2/CH_3OH (100/1, v/v) as eluent to afford compound **3** as a brown solid (167 mg, 32%). Mp: >300 °C. ^{1}H NMR ($CDCl_3$, 300 MHz) δ: 7.12 (dd, 2H, J_1 = 6.0 Hz, J_2 = 3.0 Hz), 7.37 (t, 2H, J = 9.0 Hz), 7.53−7.56 (m, 4H), 7.59−7.63 (m, 10H), 7.90−7.97(m, 6H), 9.24 (s, 2H). ^{13}C NMR ($CDCl_3$, 75 MHz) δ: 121.2, 126.1, 126.0, 126.3, 127.0, 127.2, 127.5, 128.2, 129.1, 129.5, 129.6, 129.7, 130.9, 131.6, 132.2, 133.9, 137.2, 139.8, 141.5, 152.3. HRMS (ESI-TOF) m/z: $[M + H]^+$ calcd for $C_{46}H_{27}N_2S_2$:671.1616, found 671.1608. Anal. Calcd for $C_{46}H_{26}N_2S_2$: C, 82.36; H, 3.91; N, 4.18. Found: C, 82.28; H, 4.13; N, 4.23.

■ ASSOCIATED CONTENT

Ⓢ Supporting Information

CIF files of compounds **1**−**3**, related figures, and original ^{1}H NMR, ^{13}C NMR, and HR-MS spectra. This material is available free of charge via the Internet at http://pubs.acs.org.

■ AUTHOR INFORMATION

Corresponding Author

*E-mail: qczhang@ntu.edu.sg.

Notes

The authors declare no competing financial interest.

■ ACKNOWLEDGMENTS

Q.Z. acknowledges financial support from AcRF Tier 1 (RG 16/12) and Tier 2 (ARC 20/12 and ARC 2/13) from MOE and the CREATE program (Nanomaterials for Energy and Water Management) from NRF.

■ REFERENCES

(1) (a) Zade, S. S.; Bendikov, M. *Angew. Chem., Int. Ed.* **2010**, *49*, 4012. (b) Anthony, J. E. *Angew. Chem., Int. Ed.* **2008**, *47*, 452. (c) Bendikov, M.; Wudl, F.; Perepichka, D. F. *Chem. Rev.* **2004**, *104*, 4891. (d) Anthony, J. E. *Chem. Rev.* **2006**, *106*, 5028.

(2) (a) Zhang, C.-R.; Coropceanu, V.; Sears, J. S.; Brédas, J.-L. *J. Phys. Chem. C* **2014**, *118*, 154. (b) Jiang, D.; Dai, S. *J. Phys. Chem. A* **2008**, *112*, 332K. (c) Houk, N.; Lee, P. S.; Nenel, M. *J. Org. Chem.* **2001**, *66*, 5517. (d) Bendikov, M.; Duong, H. M.; Starkey, K.; Houk, K. N.; Carter, E. A.; Wudl, F. *J. Am. Chem. Soc.* **2004**, *126*, 7416.

(3) (a) Watanabe, M.; Chang, Y. J.; Liu, S.-W.; Chao, T.-H.; Gota, K.; Islam, M. M.; Yuan, C.-H.; Tao, Y.-T.; Shinmyozu, T.; Chow, T. J. *Nat. Chem.* **2012**, *4*, 574. (b) Purushothaman, B.; Bruzek, M.; Parkin, S. R.; Miller, A.-F.; Anthony, J. E. *Angew. Chem., Int. Ed.* **2011**, *50*, 7013. (c) Tönshoff, C.; Bettinger, H. F. *Angew. Chem., Int. Ed.* **2010**, *49*, 4125. (d) Kaur, I.; Jazdzyk, M.; Stein, N. N.; Prusevich, P.; Miller, G. P. *J. Am. Chem. Soc.* **2010**, *132*, 1261. (e) Kaur, I.; Stein, N. N.; Kopreski, R. P.; Miller, G. P. *J. Am. Chem. Soc.* **2009**, *131*, 3424. (f) Chun, D.; Cheng, Y.; Wudl, F. *Angew. Chem. Int. Ed.* **2008**, *47*, 8380. (g) Payne, M. M.; Parkin, S. R.; Anthony, J. E. *J. Am. Chem. Soc.* **2005**, *127*, 8028.

(4) (a) Pascal, R. A., Jr. *Chem. Rev.* **2006**, *106*, 4809. (b) Lu, J.; Ho, D. M.; Vogelaar, N. J.; Kraml, C. M.; Pascal, R. A., Jr. *J. Am. Chem. Soc.* **2004**, *126*, 11168. (c) Qiao, X.; Ho, D. M.; Pascal, R. A., Jr. *Angew. Chem., Int. Ed.* **1997**, *36*, 1531.

(5) Duong, H. M.; Bendikov, M.; Steiger, D.; Zhang, Q.; Sonmez, G.; Yamada, J.; Wudl, F. *Org. Lett.* **2003**, *5*, 4433.

(6) (a) Zhang, Q.; Divayana, Y.; Xiao, J.-C.; Wang, Z.; Tiekink, E. R. T.; Doung, H. M.; Zhang, H.; Boey, F.; Sun, X.-W.; Wudl, F. *Chem.—Eur. J.* **2010**, *16*, 7422. (b) Xiao, J.-C.; Divayana, Y.; Zhang, Q.-C.; Doung, H.-M.; Zhang, H.; Boey, F.; Sun, X. W.; Wudl, F. *J. Mater. Chem.* **2010**, *20*, 8167. (c) Xiao, J. C.; Duong, H. M.; Liu, Y.; Shi, W. X.; Ji, L.; Li, G.; Li, S. Z.; Liu, X. W.; Ma, J.; Wudl, F.; Zhang, Q. *Angew. Chem., Int. Ed.* **2012**, *51*, 6094.

(7) For recent reviews, see: (a) Bunz, U. H. F. *Chem.—Eur. J.* **2009**, *15*, 6780. (b) Bunz, U. H. F.; Engelhart, J. U.; Lindner, B. D.; Schaffroth, M. *Angew. Chem., Int. Ed.* **2013**, *52*, 3810. (c) Bunz, U. H. F. *Pure Appl. Chem.* **2010**, *82*, 953. (d) Maio, Q. *Synlett* **2012**, 326.

(8) (a) Lindner, B. D.; Engelhart, J. U.; Tverskoy, O.; Appleton, A. L.; Rominger, F.; Peters, A.; Himmel, H. J.; Bunz, U. H. F. *Angew. Chem.Int. Ed.* **2011**, *50*, 8588. (b) Tverskov, O.; Rominger, F.; Peters, A.; Himmel, H. J.; Bunz, U. H. F. *Angew. Chem., Int. Ed.* **2011**, *50*, 3557. (c) Appleton, A. L.; Brombosz, S. M.; Barlow, S.; Sears, J. S.; Bredas, J. L.; Marder, S. R.; Bunz, U. H. F. *Nat. Commun.* **2010**, *1*, 91.

(9) (a) Miao, Q.; Nguyen, T. Q.; Someya, T.; Blanchet, G. B.; Nuckolls, C. *J. Am. Chem. Soc.* **2003**, *125*, 10284. (b) Liu, D. Q.; Xu, X. M.; Su, Y. R.; He, Z. K.; Xu, J. B.; Miao, Q. *Angew. Chem.Int. Ed.* **2013**, *52*, 6222. (c) Liang, Z. X.; Tang, Q.; Mao, R. X.; Liu, D. Q.; Xu, J. B.; Miao, Q. *Adv. Mater.* **2011**, *23*, 5514. (d) Liang, Z. X.; Tang, Q.; Xu, J. B.; Miao, Q. *Adv. Mater.* **2011**, *23*, 1535. (e) Tang, Q.; Liang, Z. X.; Liu, J.; Xu, J. B.; Miao, Q. *Chem. Commun.* **2010**, *46*, 2977.

(10) (a) Li, J.-B.; Gao, J.-K.; Li, G.; Xiong, W.-W.; Zhang, Q. *J. Org. Chem.* **2013**, *78*, 12760. (b) Gu, P.-Y.; Zhou, F.; Gao, J. K.; Li, G.; Wang, C.-Y.; Xu, Q.-F.; Zhang, Q.; Lu, J.-M. *J. Am. Chem. Soc.* **2013**, *135*, 14086. (c) Li, G.; Wu, Y.-C.; Gao, J.-K.; Wang, C.-Y.; Li, J.-B.; Zhang, H.-C.; Zhao, Y.-L.; Zhang, Q. *J. Am. Chem. Soc.* **2012**, *134*, 20298.

(11) (a) More, S.; Bhosale, R.; Choudhary, S.; Mateo-Alonso, A. *Org. Lett.* **2012**, *14*, 4170. (b) Kulisic, N.; More, S.; Mateo-Alonso, A. *Chem. Commun.* **2011**, *47*, 514. (c) Mateo-Alonso, A.; Kulisic, N.; Valenti, G.; Marcaccio, M.; Paolucci, F.; Prato, M. *Chem.—Asian J.* **2010**, *5*, 482.

(12) (a) Liu, Y. Y.; Song, C. L.; Zeng, W. J.; Zhou, K. G.; Shi, Z. F.; Ma, C. B.; Yang, F.; Zhang, H. L.; Gong, X. *J. Am. Chem. Soc.* **2010**, *132*, 16349. (b) Song, C. L.; Ma, C. B.; Yang, F.; Zeng, W. J.; Zhang, H. L.; Gong, X. *Org. Lett.* **2011**, *13*, 2880. (c) Gao, B.; Wang, M.; Cheng, Y.; Xiang, L.; Jing, X.; Wang, F. *J. Am. Chem. Soc.* **2008**, *130*, 8297.

(13) Gao, J.; Zhang, Q. *Israel J. Chem.* **2014**, DOI: 10.1002/ijch.201400003.

(14) (a) Cui, S.; Liu, H. B.; Gan, L. B.; Li, Y. L.; Zhu, D. B. *Adv. Mater.* **2008**, *20*, 2918. (b) Yang, B.; Xiao, J.-C.; Wong, J.-I.; Guo, J.; Wu, Y.-C.; Ong, L.-J.; Lao, L.-L.; Boey, F.; Zhang, H.; Yang, H.-Y.; Zhang, Q. *J. Phys. Chem. C* **2011**, *115*, 7924.

(15) (a) Liu, Y. Q.; Zhang, F.; He, C. Y.; Wu, D. Q.; Zhuang, X. D.; Xue, M. Z.; Liu, Y. G.; Feng, X. L. *Chem. Commun.* **2012**, *48*, 4166. (b) Schmidt, K.; Brovelli, S.; Coropceanu, V.; Beljonne, D.; Cornil, J.; Bazzinim, C.; Caronna, T.; Tubino, R.; Meinardi, F.; Shuai, Z. G.; Brénardi, F. *J. Phys. Chem. A* **2007**, *111*, 10490.

(16) Eastman, J. W. *Photochem. Photobiol.* **1967**, *6*, 55.

(17) (a) Hehre, W. J.; Ditchfie, R.; Pople, J. A. *J. Chem. Phys.* **1972**, *56*, 2257. (b) Becke, A. D. *J. Chem. Phys.* **1993**, *98*, 5648.

(18) (a) Liu, H. B.; Zhao, Q.; Li, Y. L.; Liu, Y.; Lu, F. S.; Zhuang, J. P.; Wang, S.; Jiang, L.; Zhu, D. B.; Yu, D. P.; Chi, L. F. *J. Am. Chem. Soc.* **2005**, *127*, 1120. (b) Guo, Y. B.; Tang, Q. X.; Liu, H. B.; Zhang, Y. J.; Li, Y. L.; Hu, W. P.; Wang, S.; Zhu, D. B. *J. Am. Chem. Soc.* **2008**, *130*, 9198.

(19) (a) Xiao, J. C.; Xiao, X. Y.; Zhao, Y. L.; Wu, B.; Liu, Z. Y.; Zhang, X. M.; Wang, S. J.; Zhao, X. H.; Liu, L.; Jiang, L. *Nanoscale* **2013**, *5*, 5420. (b) Lin, Z. Q.; Sun, P. J.; Tay, Y. Y.; Liang, J.; Liu, Y.; Shi, N. E.; Xie, L. H.; Yi, M. D.; Qian, Y.; Fan, Q. L.; Zhang, H.; Hng, H. H.; Ma, J.; Zhang, Q.; Huang, W. *ACS Nano* **2012**, *6*, 5309.

(20) (a) Xiao, J.; Yin, Z.; Li, H.; Zhang, Q.; Boey, F.; Zhang, H.; Zhang, Q. *J. Am. Chem. Soc.* **2010**, *132*, 6926. (b) Gan, H. Y.; Liu, H.

B.; Li, Y. J.; Zhao, Q.; Li, Y. L.; Wang, S.; Jiu, T. G.; Wang, N.; He, X. R.; Yu, D. P.; Zhu, D. B. *J. Am. Chem. Soc.* **2005**, *127*, 12452.
(21) Henley, S. J.; Mollah, S.; Giusca, C. E.; Silva, S. R. P. *J. Appl. Phys.* **2009**, *106*, 064309.
(22) Usui, H. *Electrochim. Acta* **2011**, *56*, 3934.
(23) Liu, H. B.; Xu, J. L.; Li, Y. J.; Li, Y. L. *Acc. Chem. Res.* **2010**, *43*, 1496.
(24) (a) Lee, S. M.; Jun, Y. W.; Cho, S. N.; Cheon, J. *J. Am. Chem. Soc.* **2002**, *124*, 11244. (b) Fu, H.; Xiao, D.; Yao, J.; Yang, G. *Angew. Chem., Int. Ed.* **2003**, *42*, 2883. (c) Tao, A. R.; Habas, S.; Yang, P. *Small* **2008**, *4*, 310.
(25) (a) MaRae, E. G.; Kasha, M. *Physical Processes in Radiation Biology*; Academic Press: New York, 1964. (b) Lee, T. W.; Park, O. O. *Adv. Mater.* **2000**, *12*, 801.
(26) Shi, J.; Chang, N.; Li, C.; Mei, J.; Deng, C.; Luo, X.; Liu, Z.; Bo, Z.; Dong, Y. Q.; Tang, B. Z. *Chem. Commun.* **2012**, *48*, 10675.
(27) (a) Hong, Y. N.; Lam, J. W. Y.; Tang, B. Z. *Chem. Commun.* **2009**, 4332. (b) Yuan, W. Z.; Lu, P.; Chen, S. M.; Lam, J. W. Y.; Wang, Z. M.; Liu, Y.; Kwok, H. S.; Ma, Y. G.; Tang, B. Z. *Adv. Mater.* **2010**, *22*, 2159.